Decay of the distance autocorrelation and Lyapunov exponents

C. F. O. Mendes,[1] R. M. da Silva,[1] and M. W. Beims[1,2]
[1]*Departamento de Física, Universidade Federal do Paraná, 81531-980 Curitiba, PR, Brazil*
[2]*Max-Planck Institute for the Physics of Complex Systems, Nöthnitzer Strasse 38, 01187 Dresden, Germany*

(Received 8 February 2019; published 7 June 2019)

This work presents numerical evidence that for discrete dynamical systems with one positive Lyapunov exponent the decay of the distance autocorrelation is always related to the Lyapunov exponent. Distinct decay laws for the distance autocorrelation are observed for different systems, namely, exponential decays for the quadratic map, logarithmic for the Hénon map, and power-law for the conservative standard map. In all these cases the decay exponent is close to the positive Lyapunov exponent. For hyperchaotic conservative systems the power-law decay of the distance autocorrelation is not directly related to any Lyapunov exponent.

DOI: 10.1103/PhysRevE.99.062206

I. INTRODUCTION

The understanding of decay of correlations in dynamical systems is of crucial relevance in nonequilibrium statistical physics. It may furnish the qualitative and quantitative knowledge about, for example, relaxation processes in complex systems [1]. In such complex systems a chaotic behavior is common, and a relation between the decay of correlations with positive Lyapunov exponents (LEs) is intuitively expected. From the theoretical point of view such a relation was studied using the standard autocorrelation function between two observables, such as in one-dimensional (1D) dissipative systems [2–4], in area-preserving maps [5], and in two-dimensional (2D) maps [2] with random perturbations [6], and conjectured that for higher-dimensional systems the smallest positive LE is an upper bound for the decay of correlation [7].

In this work we study the decay of a more recently [8] proposed correlation, called the *distance correlation* or *covariance correlation*. It was proposed for testing joint independence of random vectors in arbitrary dimensions and has received attention in applied statistics [9–13], in quantum-classical transitions analysis for ratchet systems [14], in genetic risk problems [15], and in functional brain connectivity [16] and for the parameter identification of nonlinear systems [17]. It was shown recently [18] that the distance correlation is able to detect noise-induced escape times from regular and chaotic attractors, to describe mixing properties between chaotic trajectories, and to detect properties related to the linear stability of orbital points. However, no direct relation to the LE was achieved.

The crucial issue is to extract from the distance correlation relevant properties related to nonlinear dynamics hidden in time series. Inspired by this, the present work aims to give a qualitative and quantitative connection between the distance correlation and LEs. Being more specific, we show that the positive LE is closely related to the decay of the distance correlation calculated between the time series and itself delayed in time, called here *distance autocorrelation* (D_A). Results are presented for two dissipative maps, the quadratic and the Hénon maps, and for the conservative standard map and coupled standard maps. Distinct qualitative decays of D_A as a function of the delay time Δt are observed for these maps, ranging from exponential and logarithm to power-law. In all cases the decay exponents are close to the LEs. Exceptions occur only for hyperchaotic systems.

It is widely known that the qualitative decay of Poincaré recurrence time statistics (RTS) is related to stickiness and chaotic motion found in 2D conservative systems [19,20]. As shown by numerical experiments, and described by some models, while exponential decays are observed for completely chaotic systems, power-law decays occur when the phase-space dynamics is mixed, generating the sticky motion and memory effects [21]. Such decays are expected to have generic properties. For higher-dimensional systems this is an actual debate [22,23]. The present work gives a completely new insight in this direction when considering 2D conservative systems. We have found a correlation which not only detects exponential and power-law decays, but also relates them directly to the positive LE. Thus, besides the interest in generic properties of decay of correlations, our results enable us to extract relevant quantities of dynamical systems directly from the time series.

The paper is organized as follows. In Sec. II we review the general definition of the distance correlation, and Sec. III describes the D_A used in this work. Section IV shows how the D_A can be used to determine the periodicity of a time series, and Sec. V shows its relation to the LEs from the quadratic map. In Sec. VI we test our findings for higher-dimensional systems, namely, the Hénon map and (coupled) standard maps. Section VII summarizes our main results.

II. DISTANCE CORRELATION

In this section we summary the main properties of the distance correlation [8] as a statistical measure of dependence between random vectors which is based on Euclidean distances. We present here only the computational procedure to determine the distance correlation. For more details about this procedure and original definitions we refer readers to Ref. [8].

Assume two random samples $(\boldsymbol{X},\boldsymbol{Y}) = \{(X_k, Y_k) : k = 1,\ldots,N\}$ for $N \geqslant 2$ and $X \in \mathbb{R}^s$, $Y \in \mathbb{R}^t$ with s and t integers. The *empirical distance correlation* is given by the expression

$$D_C^{(N)}(\boldsymbol{X},\boldsymbol{Y}) = \frac{\sigma_N(\boldsymbol{X},\boldsymbol{Y})}{\sqrt{\sigma_N(\boldsymbol{X})\sigma_N(\boldsymbol{Y})}}, \tag{1}$$

where the *empirical distance covariance* $\sigma_N(\boldsymbol{X},\boldsymbol{Y})$ for a joint random sample $(\boldsymbol{X},\boldsymbol{Y})$ is defined by the expression

$$\sigma_N(\boldsymbol{X},\boldsymbol{Y}) = \frac{1}{N}\left(\sum_{i,j=1}^{N} A_{ij}B_{ij}\right)^{1/2}, \tag{2}$$

where A and B are matrices. The *empirical distance variance* for a random sample $\boldsymbol{X}$ is given by

$$\sigma_N(\boldsymbol{X}) = \frac{1}{N}\left(\sum_{i,j=1}^{N} A_{ij}^2\right)^{1/2}, \tag{3}$$

and for a random sample $\boldsymbol{Y}$

$$\sigma_N(\boldsymbol{Y}) = \frac{1}{N}\left(\sum_{i,j=1}^{N} B_{ij}^2\right)^{1/2}. \tag{4}$$

For $X \in \mathbb{R}^s$ with $i = 1,\ldots,N$ and $j = 1,\ldots,N$, the matrix A is obtained from

$$A_{ij} = a_{ij} - \bar{a}_{i.} - \bar{a}_{.j} + \bar{a}_{..}, \tag{5}$$

where $a_{ij} = |X_i - X_j|$ is the Euclidean norm of the distance between the elements of the sample, $\bar{a}_{i.} = \frac{1}{N}\sum_{j=1}^{N} a_{ij}$ and $\bar{a}_{.j} = \frac{1}{N}\sum_{i=1}^{N} a_{ij}$ are the arithmetic mean of the rows and columns, respectively, and $\bar{a}_{..} = \frac{1}{N^2}\sum_{i,j=1}^{N} a_{ij}$ is the general mean. Similarly to $Y \in \mathbb{R}^t$ defined by $i = 1,\ldots,N$ and $j = 1,\ldots,N$, we also define the matrix

$$B_{ij} = b_{ij} - \bar{b}_{i.} - \bar{b}_{.j} + \bar{b}_{..}, \tag{6}$$

where the terms b_{ij}, $\bar{b}_{i.}$, $\bar{b}_{.j}$, and $\bar{b}_{..}$ are similar to those for the matrix A_{ij}.

The $D_C^{(N)}(\boldsymbol{X},\boldsymbol{Y})$ is defined inside the interval [0,1] and its main characteristic is that it will be zero if and only if the random vectors are independent [8–12]. In addition, it is easy to check that $D_C^{(N)}(\boldsymbol{X},\boldsymbol{Y})$ is scale independent. This means that samples $\boldsymbol{X}$ and $\boldsymbol{Y}$ can be multiplied by α and β, with $\alpha,\beta \in \mathbb{R}$, and $D_C^{(N)}(\boldsymbol{X},\boldsymbol{Y})$ remains unaltered. The $D_C^{(N)}(\boldsymbol{X},\boldsymbol{Y})$ requires only a series of data in order to be analyzed. This can be crucial when analyzing experimental data.

III. DISTANCE AUTOCORRELATION

Defining matrix B to be equal to matrix A with a delay Δt, the matrix elements are related by $B_{i,j} = A_{i+\Delta t, j+\Delta t}$. In the present work we always consider time series, so that Δt is a time delay. Using increasing values of Δt this is a discrete convolution between A and $A_{i+\Delta t, j+\Delta t}$, and we expect to obtain some relevant information about the dynamics of the original time series as a function of Δt. In other words, for the calculation of D_A, we use here only *one* time series of states of a particular initial condition (IC) to compose the sample $\{\boldsymbol{X}\}$. From this time series, we obtain the data set $\{\boldsymbol{Y}\}$ by only shifting the states of $\{\boldsymbol{X}\}$ on time. Thus, we must consider the following representation for the joint sequence $(\boldsymbol{X},\boldsymbol{Y})$:

$$\boldsymbol{X} \Rightarrow (X_n : X_1, X_2, X_3, \ldots, X_N),$$
$$\boldsymbol{Y} = \boldsymbol{X'} \Rightarrow (X_n : X_{1+\Delta t}, X_{2+\Delta t}, X_{3+\Delta t}, \ldots, X_{N+\Delta t}).$$

Here n is an integer referring the times for which the variables $(\boldsymbol{X},\boldsymbol{Y})$ were determined. For maps, $1 \leqslant \Delta t \leqslant N$ is a positive integer. Thus, the distance autocorrelation function is then defined by

$$D_A = D_C^{(N)}(\boldsymbol{X},\boldsymbol{X'}) = \frac{\sigma_N(\boldsymbol{X},\boldsymbol{X'})}{\sqrt{\sigma_N(\boldsymbol{X})\sigma_N(\boldsymbol{X'})}}. \tag{7}$$

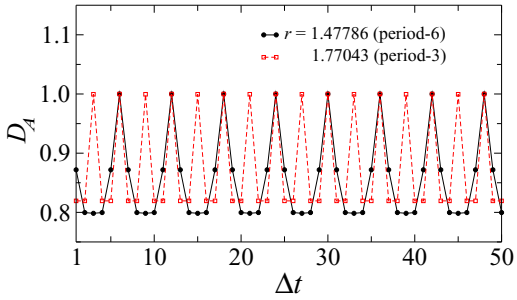

FIG. 1. D_A as a function of Δt for the QM (8) considering two periodic windows: $r = 1.47786$ (period-6) and $r = 1.77043$ (period-3).

IV. DETECTING PERIODICITY

It is easy to realize that the D_A calculated between samples $\boldsymbol{X}$ and $\boldsymbol{X'}$ will be $D_A = 1$ when $\Delta t = m$, with m being the periodicity of the time series. To check this obvious property we present numerically results only for one time discrete dynamical system, the quadratic map.

Quadratic map (QM). The quadratic map is a 1D dynamical system given by the expression [24,25]

$$x_{n+1} = r - x_n^2, \tag{8}$$

where r is a control parameter that belongs to the range $[-0.25, 2]$, $n = 0, 1, 2, 3, \ldots$ the integer which represents the number of iterations, and $x_n \in [-2, 2]$ is the state of the system at time n. Results for D_A as a function of Δt are presented in Fig. 1. D_A is shown for two periodic windows located at the parameters $r = 1.47786$ (period-6) and $r = 1.77043$ (period-3). We notice that in both cases $D_A = 1$ when $\Delta t = 6$ and $\Delta t = 3$, respectively. This means that D_A furnishes a measure of how much the time series repeats itself. Since this is an evident property we will not show it in other dynamical systems.

V. RELATION TO LYAPUNOV EXPONENTS

In this section we show that the D_A calculated in Sec. III is related to the maximal LE. We mention that while the LE gives the exponential divergence of nearby trajectories in the linear approximation, the D_A may contain in itself nonlinear extensions of this property and is not restricted to furnishes solely the usual LE.

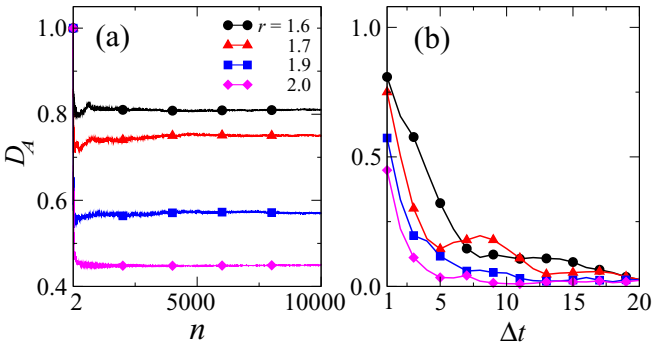

FIG. 2. (a) Time evolution of D_A for four parameters corresponding to the chaotic regime of the QM (8). The parameters are $r = 1.6$, 1.7, 1.9, and 2.0. The IC used is $x_0 = 0.1$, and the displacement of the states between the samples is $\Delta t = 1$. (b) D_A as a function of Δt for the same parameters from panel (a).

To start the discussion we first have to guarantee that the D_A converges to a reasonable value for a given Δt. This is presented in Fig. 2(a) for the QM with $r = 1.6$, 1.7, 1.9, and 2.0. In this case, $\Delta t = 1$. This shows that for each value of r the D_A converges asymptotically, as a function of n, to distinct finite values. In other words, even for a chaotic trajectory, D_A does not converges to zero. Such situation changes drastically when $D_C^{(N)}(\boldsymbol{X}, \boldsymbol{Y})$ is calculated between two distinct ICs inside the chaotic regime. This leads to mixing properties for which $D_C^{(N)}(\boldsymbol{X}, \boldsymbol{Y})$ tends to zero with $n^{-1/2}$, as shown in Ref. [18].

The next step is to show how such asymptotic values of D_A change with Δt. This is presented in Fig. 2(b), which displays D_A as a function of Δt for parameters inside the chaotic regimes of the QM, namely, $r = 1.6$, 1.7, 1.9, and 2.0. No values $D_A = 1$ are observed since the chaotic trajectory is not periodic anymore. We note that all D_A curves converge to small, but finite, values when $\Delta t = 20$.

From Fig. 2(a) we observe that when we increase r the corresponding D_A decrease. Even though we expect that for time series with larger LEs the D_A is smaller, we wonder if there is an analytical relation between both. To find such a relation we first determine D_A for many values of parameters inside the interval $1.25 \leqslant r \leqslant 2.0$ of the QM. This is shown in Fig. 3(a). In this case we considered just two time delays, $\Delta t = 1$ (blue curve) and $\Delta t = 2$ (orange curve), from a total iteration time of $n = 10^4$. A direct comparison between D_A and the LE (λ) from the QM, shown in Fig. 3(b), allows us to realize that, besides the regions with periodic motion, D_A decreases while λ increases with the increment of r. It becomes clear that D_A is able to identify the periodic windows that occur at specific values of r.

Now we combine data for D_A from Fig. 3(a) with those for λ from Fig. 3(b). This is plotted in Fig. 4 and shows the relation between the LE and D_A for $\Delta t = 1$, 2. Clearly almost all positive LEs belong to decreasing lines when increasing D_A. Linear adjusted lines are given in the inset of this figure. Since the above analysis depends on the specific Δt used, it is not appropriate to extract general nonlinear properties from D_A. Thus, we move forward and argue that there should exist some relation between the LEs and the time decay of D_A as a function of Δt. This argument is reasonable due to the fact

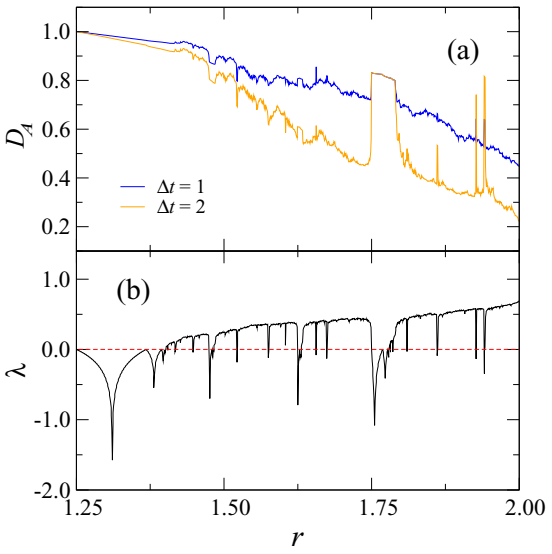

FIG. 3. (a) D_A for $\Delta t = 1$ (blue) and $\Delta t = 2$ (orange) and (b) LE, both as a function of r. The initial condition used is $x_0 = 0.1$, and the parameter r is divided into 10^3 equally spaced parts.

that the D_A calculated for the time series with itself for distinct values of Δt is related to the convolution between both series.

To check this, we obtained the samples $\{\boldsymbol{X} = X_n : x_1, x_2, \ldots, x_N\}$ and $\{\boldsymbol{X'} = X_n : x_{1+\Delta t}, x_{2+\Delta t}, \ldots, x_{N+\Delta t}\}$ by iterating the QM (8) $n = 10^4$ times after discarding the first 5×10^3 transitory iterations. To determine the D_A we calculate an average over 5×10^3 ICs randomly chosen with equal probability inside the interval $[-2, 2]$ to reach a satisfactory level of accuracy in the asymptotic D_A values. We write the mean distance autocorrelation as $\langle D_A \rangle$. Figure 5 shows $\langle D_A \rangle$ (red circles) as a function of Δt in semilog scale for three different values of the parameter r in the chaotic regime. We consider the displacement only in the interval $1 \leqslant \Delta t \leqslant 10$. In Fig. 5(a) we display the case $r = 1.7$, which has a LE $\lambda = 0.438$. In Figs. 5(b) and 5(c) the cases $r = 1.9$ and $r = 2.0$ are shown, for which $\lambda = 0.548$ and $\lambda = 0.693$ are found,

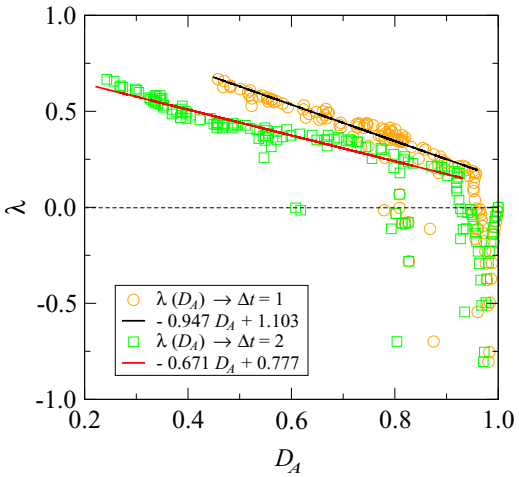

FIG. 4. LE as a function of D_A for the cases $\Delta t = 1$ and $\Delta t = 2$. The functions for the adjustments are given in the inset.

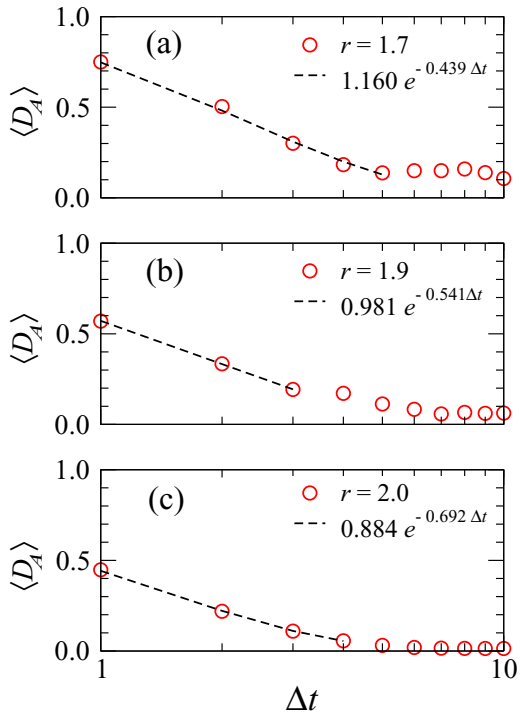

FIG. 5. Curves plotted in semilog scale of the $\langle D_A \rangle$ as a function of Δt for (a) $r = 1.7$, (b) $r = 1.9$, and (c) $r = 2.0$. The functions for the adjustments (dashed black lines) are given in the panels.

respectively. Straight lines in these curves can be fitted by exponential decays of the type $\langle D_A \rangle \propto \alpha \exp(-\beta \Delta t)$, where α and β are adjustment parameters. Remarkably, the parameters $\beta = 0.439$, $\beta = 0.541$, and $\beta = 0.692$ provide similar values as the corresponding LEs $\lambda = 0.438$, $\lambda = 0.548$, and $\lambda = 0.693$, as can be observed from the adjusted curves (dashed black line) in Fig. 5. We have checked the relation $\beta \approx \lambda$ for other parameters of the QM. This is displayed in Fig. 6(a), which shows the LE λ (continuous black line) and β (circles)

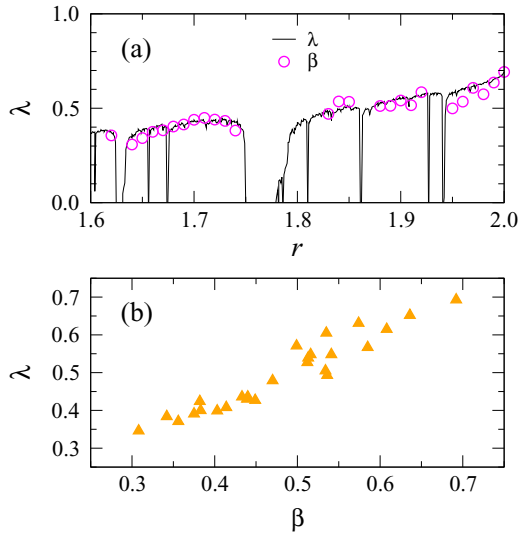

FIG. 6. (a) LE and the adjustment parameter β in function of r and (b) the relationship between λ and β.

as a function of r. From this figure, we can conclude that the relation $\beta \approx \lambda$ is valid for the values of r that lead to chaotic dynamics. Figure 6(b) combines data for λ and β in the plane $\lambda \times \beta$. These results show that the decay of D_A as a function of Δt is closely related to the LE of the dynamical system. We have also tried to increase the number of samples, i.e., iteration n and ICs, but no relevant changes were observed.

Additional simulations (not shown) were performed for the Bernoulli shift and the Baladi map [26]. Both are simple linear maps. While for the Bernoulli shift the D_A decays exponentially with the LE ($\lambda \sim 0.69$), for the Baladi map no relation with the LE was found. In the latter map, the LE is not even related to the usual decay of correlations (see Ref. [26] for more details).

VI. EXTENSION TO HIGHER-DIMENSIONAL SYSTEMS

In the following we analyze the relation of the decay of D_A with the LE in nonlinear systems with more dimensions. We start with the dissipative Hénon map and then consider the conservative (coupled) standard map.

Hénon map (HM). The Hénon map is a generalization of the quadratic map for 2D systems, and it is given by [27]

$$\begin{aligned} x_{n+1} &= r - x_n^2 + b y_n, \\ y_{n+1} &= x_n. \end{aligned} \tag{9}$$

The additional parameter b determines the dissipation of the system. The HM is dissipative for $|b| < 1$. This 2D map has two LEs. It is well known that the HM has a chaotic attractor for $r = 1.4$ and $b = 0.3$ [27] with positive LE $\lambda = 0.418$. Figure 7(a) displays the finite time LE as a function of the iteration. For $n = 9000$ it converges to $\lambda = 0.418$. Since we are considering two dimensions, the quantities for D_A are obtained from $|X_i - X_j| = \sqrt{(x_i - x_j)^2 + (y_i - y_j)^2}$. Results are displayed in Fig. 7(b) and show the corresponding behavior of D_A. When we refer to the adjusted curve we use the notation $D_A(\Delta t)$. As seen in this figure, the decay of D_A is well adjusted by the function $D_A(\Delta t) \sim 0.956 - 0.419 \ln(\Delta t)$. Thus the time decay coefficient 0.419 is close to the LE $\lambda = 0.418$.

Standard map (SM). Here we consider the 2D conservative SM given by [28]

$$\begin{aligned} p_{n+1} &= p_n + K \sin(2\pi x_n) \quad [\text{mod } 1], \\ x_{n+1} &= x_n + p_{n+1} \quad [\text{mod } 1], \end{aligned} \tag{10}$$

where x_n is the position at the iteration $n = 0, 1, 2, \ldots$, and p_n its conjugated momentum. K is the nonlinear positive parameter, and its value determines the topology of the phase space. Some values of K lead to a mixed phase space compound by Kolmogorov-Arnold-Moser tori and a stochastic region [29]. The chaotic trajectory can be trapped for long, but finite, times close to the tori, giving an origin to the *stickiness effect* [30]. This scenario can be obtained using $K = 0.57$, for which $\lambda = 0.750$, as shown by the time evolution of the finite time LE in Fig. 7(c). A totally chaotic phase space takes place if $K = 1.43$, with $\lambda = 1.505$ [see Fig. 7(e)]. In both cases the appropriate adjustment was $D_A(\Delta t) \propto \alpha \Delta t^{-\beta}$. Also here the quantities for D_A are obtained from $|X_i - X_j| = \sqrt{(x_i - x_j)^2 + (p_i - p_j)^2}$. For the mixed case we have $\alpha = 0.422$ and $\beta = 0.748$, which is very close to the associated LE [see Fig. 7(d)], and for the chaotic case we found $\alpha = 0.407$

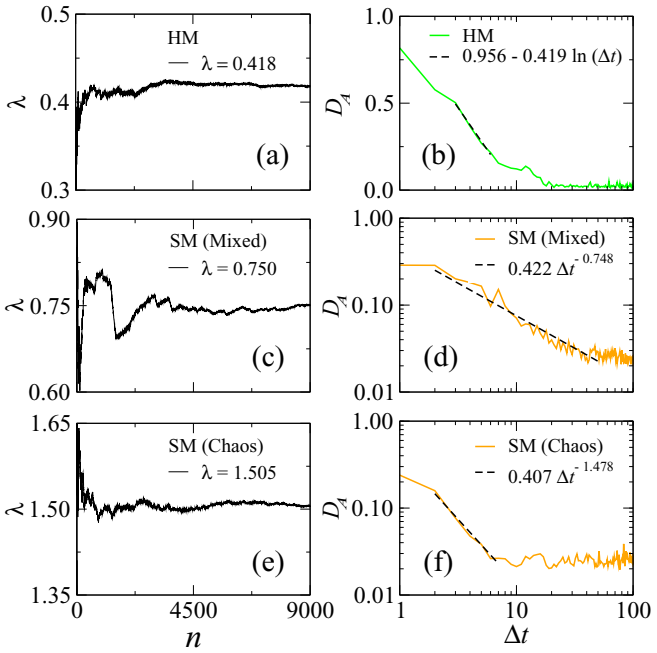

FIG. 7. (a) Finite-time LE and (b) the corresponding $D_A(\Delta t)$ (green curve) in semilog scale for the HM (9) with parameters $r = 1.4$ and $b = 0.3$. In panels (c) and (e), the finite-time LEs for the SM (10) with mixed and chaotic phase space are displayed, respectively. Panels (d) and (f) show the corresponding $D_A(\Delta t)$ (orange curve) in the log-log scale. The dashed black lines in panels (b), (d), and (f) are the associated adjustments.

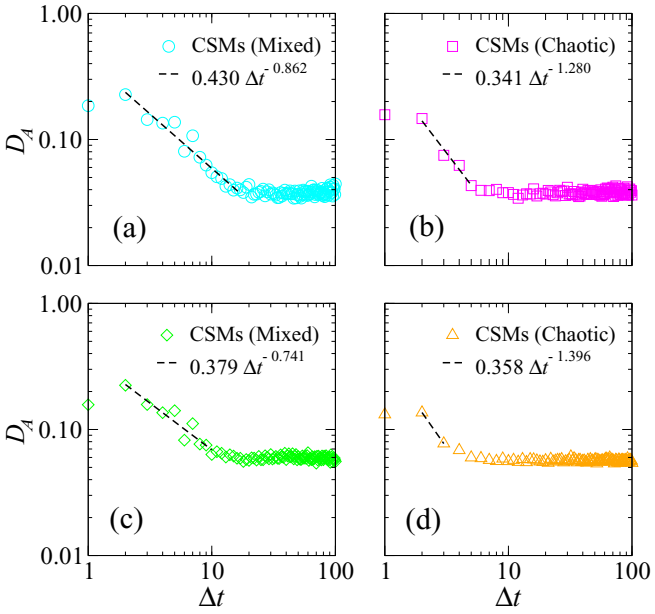

FIG. 8. $D_A(\Delta t)$ for CSMs (11)–(12) with $N = 2$ (a) for the mixed (circles in cyan) and (b) for the chaotic (squares in magenta) cases. With $N = 4$, the mixed (green diamonds) and the chaotic (orange triangles) cases are displayed in panels (c) and (d), respectively. The dashed-black lines are the associated adjustment. Results are summarized in Table I.

and $\beta = 1.478$ [Fig. 7(f)], which is also close to the respective LE $\lambda = 1.505$.

Coupled standard maps (CSMs). In this model we consider a coupling between identical conservative SMs. For our numerical investigation we used the 2D SM [31,32]:

$$\mathbf{M_i}\begin{pmatrix} p_i \\ x_i \end{pmatrix} = \begin{pmatrix} p_i + K_i \sin(2\pi x_i) & [\text{mod } 1] \\ x_i + p_i + K_i \sin(2\pi x_i) & [\text{mod } 1] \end{pmatrix}, \quad (11)$$

and for the coupling

$$\mathbf{T_i}\begin{pmatrix} p_i \\ x_i \end{pmatrix} = \begin{pmatrix} p_i + \sum_{j=1}^{N} \xi_{i,j} \sin[2\pi(x_i - x_j)] \\ x_i \end{pmatrix}, \quad (12)$$

with $\xi_{i,j} = \xi_{j,i} = \frac{\xi}{\sqrt{N-1}}$ (all-to-all coupling). This constitutes a $2N$-dimensional Hamiltonian system, and the total map is a composition of T and M. We considered two cases: (1) $N = 2$ and (2) $N = 4$, for which D_A is obtained from

$$|X_i - X_j| = \sqrt{\sum_{k=1}^{N} \left[\left(x_i^{(k)} - x_j^{(k)}\right)^2 + \left(p_i^{(k)} - p_j^{(k)}\right)^2\right]}.$$

Case (1). Here we have two positive LEs ($\lambda_1 = 0.860$ and $\lambda_2 = 0.727$) for the mixed dynamics obtained using $K_1 = 0.57$ and $K_2 = 0.59$. Calculating $D_A(\Delta t)$ for this case, we obtain $\beta = 0.862$ [see Fig. 8(a)]. Considering the chaotic case with $K_1 = 1.43$ and $K_2 = 1.45$, we have LEs $\lambda_1 = 1.563$ and $\lambda_2 = 1.469$ and the parameter that fits the decay of $D_A(\Delta t)$ is $\beta = 1.280$, as seen in Fig. 8(b). In either case the function used to the adjustment was $D_A(\Delta t) \sim \alpha \Delta t^{-\beta}$.

Case (2). Here we have four positive LEs ($\lambda_1 = 0.922, \lambda_2 = 0.853, \lambda_3 = 0.776$, and $\lambda_4 = 0.624$) for the mixed dynamics obtained with $K_1 = 0.57$, $K_2 = 0.58$, $K_3 = 0.59$, and $K_4 = 0.60$. In this case, again we found for the adjustment the function $D_A(\Delta t) = \alpha\, \Delta t^{-\beta}$, with $\beta = 0.741$, as can be seen in Fig. 8(c). For the chaotic case, obtained with $K_1 = 1.42$, $K_2 = 1.43$, $K_3 = 1.44$, and $K_4 = 1.45$, we have LEs $\lambda_1 = 1.608, \lambda_2 = 1.558, \lambda_3 = 1.500$, and $\lambda_4 = 1.437$. Results are shown in Fig. 8(d), and we obtain $\beta = 1.396$.

Results for higher-dimensional systems are summarized in Table I. The decay of D_A in higher-dimensional systems with more than one positive LE does not give precise information about the LEs. In such cases β is close to the smallest LE, a feature also observed for the autocorrelation function [7].

TABLE I. Table presents the models and corresponding positive LEs $\lambda_i (i = 1, 2, 3, 4)$ with the adjustment curves and the associated decay exponents β.

Model	λ_1	λ_2	λ_3	λ_4	β	$D_A(\Delta t)$
HM	0.418	–	–	–	0.419	$-\beta \ln(\Delta t)$
SM (mixed)	0.750	–	–	–	0.748	$0.422\, \Delta t^{-\beta}$
SM (chaotic)	1.505	–	–	–	1.478	$0.407\, \Delta t^{-\beta}$
2-CSM (mixed)	0.860	0.727	–	–	0.862	$0.430\, \Delta t^{-\beta}$
2-CSM (chaotic)	1.563	1.469	–	–	1.280	$0.341\, \Delta t^{-\beta}$
4-CSM (mixed)	0.922	0.853	0.776	0.624	0.741	$0.379\, \Delta t^{-\beta}$
4-CSM (chaotic)	1.608	1.558	1.500	1.437	1.396	$0.358\, \Delta t^{-\beta}$

VII. CONCLUSIONS

The present work analyzes numerically the relation between the decay of the distance autocorrelation and LEs. Results are shown for the dissipative quadratic and Hénon maps and for the conservative standard map and coupled standard maps. For all conservative cases we found a decay for D_A proportional to $\Delta t^{-\beta}$, where β is very close to the LE λ in the case where the system has just one positive LE. For the 1D dissipative system (quadratic map) the observed decay obeys $e^{-\beta\Delta t}$ with $\beta \sim \lambda$. For the 2D dissipative system (Hénon map), the decay follows $-\beta \ln(\Delta t)$, and $\beta \sim \lambda$. Thus, for systems with one positive LE the decay of the distance autocorrelation is nicely related to the LE. Based on the knowledge about the relationship between power-law (exponential) decays of the RTS with sticky (chaotic) motion, we can conjecture that power-law decays of the D_A are also related to sticky motion. Furthermore, better than the RTS, apparently the D_A can also detect tiny sticky effects in a fully chaotic conservative system. Memory effects can occur in fully chaotic conservative systems, as shown in Ref. [21], where a completely distinct procedure was used to detect memory effects.

Further investigations will study in more detail the decay of D_A in hyperchaotic and in time-continuous systems. Moreover, it should be possible to extract from D_A more general aspects of the dynamics, since D_A certainly contains information which goes beyond the linear stability analysis of the exponential divergence of trajectories, quantified by the LE.

ACKNOWLEDGMENTS

C.F.O.M. thanks FAPEAM, R.M.d.S. thanks CAPES, and M.W.B. thanks CNPq for financial support. The authors also acknowledge computational support from Prof. Carlos M. de Carvalho at LFTC-DFis-UFPR.

[1] M. Falcioni, S. Isola, and A. Vulpiani, Phys. Lett. A **144**, 341 (1990).
[2] R. Badii, K. Heinzelmann, P. F. Meier, and A. Politi, Phys. Rev. A **37**, 1323 (1988).
[3] J. Slipantschuk, O. F. Bandtlow, and W. Just, Europhys. Lett. **104**, 20004 (2013).
[4] J. Slipantschuk, O. F. Bandtlow, and W. Just, J. Phys. A **46**, 075101 (2013).
[5] J. D. Crawford and J. R. Cary, Physica D **6**, 223 (1983).
[6] A. Blumenthal, J. Xue, and L.-S. Young, Commun. Math. Phys. **359**, 347 (2018).
[7] P. Collet and J.-P. Eckmann, J. Stat. Phys. **115**, 217 (2004).
[8] G. J. Székely, M. L. Rizzo, and N. K. Bakirov, Ann. Statist. **35**, 2769 (2007).
[9] G. J. Székely and M. L. Rizzo, Ann. Appl. Stat. **3**, 1236 (2009).
[10] G. J. Székely and M. L. Rizzo, Stat. Probabil. Lett. **82**, 2278 (2012).
[11] G. J. Székely and M. L. Rizzo, J. Multivariate Anal. **117**, 193 (2013).
[12] G. J. Székely and M. L. Rizzo, Ann. Statist. **42**, 2382 (2014).
[13] G. J. Székely and M. L. Rizzo, Ann. Rev. Stat. App. **4**, 447 (2017).
[14] M. W. Beims, M. Schlesinger, C. Manchein, A. Celestino, A. Pernice, and W. T. Strunz, Phys. Rev. E **91**, 052908 (2015).
[15] J. Kong, S. Wang, and G. Wahba, Stat. Med. **34**, 1708 (2015).
[16] L. Geerligs, Cam-Can, and R. N. Henson, Neuroimage **135**, 16 (2016).
[17] J. R. Ayala Solares and H.-L. Wei, Nonlinear Dynam. **82**, 201 (2015).
[18] C. F. O. Mendes and M. W. Beims, Physica A **512**, 721 (2018).
[19] B. V. Chirikov and D. L. Shepelyanski, Physica D **13**, 395 (1984).
[20] G. Cristadoro and R. Ketzmerick, Phys. Rev. Lett. **100**, 184101 (2008).
[21] J. C. Xavier, W. T. Strunz, and M. W. Beims, Phys. Rev. E **92**, 022908 (2015).
[22] S. Lange, F. Richter, M. Onken, A. Bäcker, and R. Ketzmerick, Chaos **24**, 024409 (2014).
[23] R. M. da Silva, C. Manchein, and M. W. Beims, Phys. Rev. E **97**, 022219 (2018).
[24] K. T. Alligood, T. D. Sauer, and J. A. Yorke, *Chaos: An Introduction to Dynamical Systems* (Springer-Verlag, New York, 1996).
[25] R. Gilmore and M. Lefranc, *The Topology of Chaos: Alice in Stretch and Squeezeland* (Wiley-VCH, Weinheim, 2011).
[26] P. Collet and J.-P. Eckmann, *Concepts and Results in Chaotic Dynamics: A Short Course* (Springer-Verlag, Berlin, 2006).
[27] M. Hénon, Commun. Math. Phys. **50**, 69 (1976).
[28] B. V. Chirikov, Phys. Rep. **52**, 263 (1979).
[29] A. Lichtenberg and M. Lieberman, *Regular and Chaotic Dynamics* (Springer Verlag, Berlin, 1992).
[30] J. D. Meiss and E. Ott, Phys. Rev. Lett. **55**, 2741 (1985).
[31] E. G. Altmann and H. Kantz, Europhys. Lett. **78**, 10008 (2007).
[32] R. M. da Silva, C. Manchein, M. W. Beims, and E. G. Altmann, Phys. Rev. E **91**, 062907 (2015).